Characterization of Palladin, a Novel Protein Localized to Stress Fibers and Cell Adhesions

Mana M. Parast* and Carol A. Otey‡

*Department of Cell Biology, University of Virginia, Charlottesville, Virginia 22908; and ‡Department of Cell and Molecular Physiology, University of North Carolina at Chapel Hill, Chapel Hill, North Carolina 27599

Abstract. Here, we describe the identification of a novel phosphoprotein named palladin, which colocalizes with α-actinin in the stress fibers, focal adhesions, cell–cell junctions, and embryonic Z-lines. Palladin is expressed as a 90–92-kD doublet in fibroblasts and coimmunoprecipitates in a complex with α-actinin in fibroblast lysates. A cDNA encoding palladin was isolated by screening a mouse embryo library with mAbs. Palladin has a proline-rich region in the NH_2-terminal half of the molecule and three tandem Ig C2 domains in the COOH-terminal half. In Northern and Western blots of chick and mouse tissues, multiple isoforms of palladin were detected. Palladin expression is ubiquitous in embryonic tissues, and is downregulated in certain adult tissues in the mouse. To probe the function of palladin in cultured cells, the Rcho-1 trophoblast model was used. Palladin expression was observed to increase in Rcho-1 cells when they began to assemble stress fibers. Antisense constructs were used to attenuate expression of palladin in Rcho-1 cells and fibroblasts, and disruption of the cytoskeleton was observed in both cell types. At longer times after antisense treatment, fibroblasts became fully rounded. These results suggest that palladin is required for the normal organization of the actin cytoskeleton and focal adhesions.

Key words: focal adhesion • adherens junction • microfilament • α-actinin • trophoblast

Introduction

The actin cytoskeleton is intimately involved in cell adhesion and maintenance of cell shape. In cultured cells, actin filaments are associated with two types of junctional sites: the cell–cell adherens junctions, and the cell–matrix focal adhesions. Each type of junction possesses its own specialized transmembrane protein: integrins in focal adhesions and cadherins in adherens junctions. In the focal adhesions, the array of cytoplasmic proteins that colocalize with integrins is complex, and includes both structural proteins that bind directly to actin (such as talin, vinculin, tensin, and α-actinin), and low-abundance adapter proteins and signaling molecules (including FAK, paxillin, zyxin, and $p130^{Cas}$; Craig and Johnson, 1996; Gilmore and Burridge, 1996). A subset of these proteins is found also in the cell–cell junctions, where they associate with the cadherin–catenin complex (Aberle et al., 1996; Provost and Rimm, 1999; Gumbiner, 2000).

α-Actinin is an actin–cross-linking protein that is common to both cell–cell and cell–matrix junctions. Monomers of α-actinin form head-to-tail dimers, which are capable of organizing actin microfilaments into stable parallel bundles (Flood et al., 1995; Djinovic-Carugo et al., 1999). In organized tissues, α-actinin has been localized to a variety of junctional sites, including the dense bodies of smooth muscle and the intercalated discs of cardiac muscle. This localization pattern is consistent with the idea that α-actinin plays a highly conserved role in the stable attachment of actin filaments to the plasma membrane. α-Actinin appears to serve this role in part by binding directly to transmembrane proteins. Binding to α-actinin, either in vitro or in vivo, has been detected with a diverse group of transmembrane receptor proteins, including several different β integrin subunits (Otey et al., 1990; Pavalko and LaRoche, 1993; Sampath et al., 1998), L-selectin (Pavalko et al., 1995), ICAM-1 (Carpen et al., 1992), and the NMDA neurotransmitter receptor (Wyszynski et al., 1997).

Within the sarcomeres of striated muscle, α-actinin is concentrated in the Z-disc, where actin thin filaments are anchored. The skeletal muscle isoform of α-actinin, actinin-2, has an especially large number of binding partners, including the giant protein, titin (Ohtsuka et al., 1997; Sorimachi et al., 1998), and the recently described myotilin (Salmikangas et al., 1999), both of which contain an Ig-like domain called Ig C2. Actinin-2 also binds to three PDZ

Address correspondence to Dr. Carol Otey, Department of Cell and Molecular Physiology, CB #7545, UNC-CH, Chapel Hill, NC 27599. Tel.: (919) 966-8239. Fax: (919) 966-6927. E-mail: carol_otey@med.unc.edu

domain proteins, ALP, ZASP, and Cypher, all of which colocalize with α-actinin in the Z-line (Xia et al., 1997; Faulkner et al., 1999; Pomies et al., 1999; Zhou et al., 1999). Binding of actinin-2 to dystrophin (Hance et al., 1999) and CapZ (Papa et al., 1999) has also been reported.

In fibroblasts and many other nonmuscle cells, α-actinin is not restricted only to junctional sites, but is also found in a distinctive beads-on-a-string punctate pattern along stress fibers, which resembles the striated pattern of myofibrils (Lazarides and Burridge, 1975). In addition to α-actinin, these striations have been reported to contain vasodilator-stimulated phosphoprotein (VASP)[1] (Reinhard et al., 1992) and sometimes zyxin (Crawford et al., 1992), and its binding partner CRP (Sadler et al., 1992; Pomies et al., 1997). The significance of these stress fiber complexes in nonmuscle cells is not well understood; however, CRP family members, all of which have multiple LIM domains, have been shown to play in important role in skeletal muscle differentiation (Arber et al., 1994, 1997), and VASP has been shown to regulate actin filament organization through its interaction with profilin (Reinhard et al., 1995a; Gertler et al., 1996). Taken together, these results suggest that α-actinin may have an important role in addition to its ability to cross-link actin and to bind transmembrane proteins: it may act as an adapter molecule to organize LIM proteins, PDZ proteins, and Ig C2 proteins into functional complexes closely associated with actin filaments. The recent report that α-actinin binds to a serine–threonine kinase in the MAP kinase pathway, MEKK1, further supports the idea that α-actinin serves to integrate signaling pathways with the actin cytoskeleton (Christerson et al., 1999).

In this report, we describe the identification of a novel protein that colocalizes with α-actinin in focal adhesions, cell–cell junctions, and stress fiber striations. We propose the name palladin for this protein, in honor of the Renaissance architect Palladio, to reflect the localization of the protein to architectural elements of the cell. Palladin contains three tandem Ig C2 domains. Unlike most intracellular Ig C2-containing proteins, which are specific to skeletal muscle, palladin is detected in both muscle and nonmuscle tissues and cells. Palladin exists as multiple isoforms, some of which are expressed in a developmentally regulated pattern. Most importantly, palladin appears to play a critical role in the organization of the actin cytoskeleton and focal adhesions in cultured trophoblast and fibroblast cells.

Materials and Methods

Cell Culture

Unless otherwise stated, all cells were cultured in DME (GIBCO BRL) containing 100 U/ml penicillin G, and 100 μg/ml streptomycin (pen/strep; GIBCO BRL), and supplemented with 10% FBS (GIBCO BRL). Day-10 chick embryos were used as a source for all avian cells and tissues. Chick embryo fibroblasts (CEFs) were prepared as described previously (Hungerford et al., 1996). Cardiac myocytes were prepared from embryo hearts following the protocol of Dabiri et al. (1999). To obtain pigmented epithelium, eyes were removed from the embryo, the pigmented epithelium was teased off and placed on sterile gelatin-coated coverslips, and was cultured for 24 h. Mouse embryo fibroblasts (MEFs) were prepared from day-13–14 embryos. Both CEFs and MEFs were used in early passage (pass 3–10). CHO cells were grown in α-MEM with 10% FBS and pen/strep, and HeLa cells were grown in DME with 5% FBS, 1 mM sodium pyruvate, 0.1 mM nonessential amino acids, and 20 mM Hepes, pH 7.2. Rat choriocarcinoma (Rcho-1) stem cells were grown as described by Kamei et al. (1997). To maintain the Rcho-1 as proliferative stem cells, they were fed growth medium: NCTC-135 (Sigma-Aldrich) with 20% FBS, 1 mM sodium pyruvate, 2 mM L-glutamine, 50 μM β-mercaptoethanol, and pen/strep. To induce differentiation of Rcho-1 cells, the stem cells were lightly trypsinized for 1 min to remove the most undifferentiated cells, and the remaining cells were fed differentiation medium, which is the same as the growth medium except with 10% horse serum instead of FBS.

mAbs and Immunofluorescence

Palladin immunoprecipitated from CEFs was used as an immunogen to obtain additional mAbs. Mice were immunized with excised SDS-PAGE bands of 90-kD palladin, splenic lymphocytes were isolated, and hybridomas were obtained as described in Chang et al. (1995). Hybridoma supernatants were screened initially by ELISA for reactivity with fixed CEFs. A second screen was performed using immunofluorescence staining and Western blots of CEFs and Swiss 3T3 cells. Eight mAbs were generated, two of which were chick-specific (2D12 and 6H11) and six of which cross-reacted with mouse (1E6, 7C6, 3C9, 4D10, 8B10, and 9C12). All the mAbs produced the same staining pattern as the original C10 mAb in fixed cells and detected the same band by Western blot.

Immunofluorescence staining was performed on cells fixed in 3.7% formaldehyde and permeabilized in 0.2% Triton X-100. Antipaxillin polyclonal antibody was the gift of Dr. Michael Schaller (University of North Carolina, Chapel Hill, NC), α-actinin polyclonal antibody was the gift of Dr. Keith Burridge (University of North Carolina, Chapel Hill, NC), and antimyc mAb was the gift of Dr. Doug DeSimone (University of Virginia, Charlottesville, VA). α-Actinin monoclonal (A5044) and FITC-conjugated phalloidin were from Sigma-Aldrich. Texas red-conjugated anti-mouse antibodies were from Jackson Immunochemicals.

Triton Extraction Experiments

To fractionate cellular proteins into a soluble pool and a cytoskeleton-associated pool, the Triton extraction method was used, as previously described (Adams et al., 1996, Wulfkuhle et al., 1999). In brief, MEFs were scraped on ice in 0.5% Triton X-100 in cytoskeleton-stabilizing buffer (50 mM NaC1, 10 mM Pipes, pH 6.8, 3 mM $MgCl_2$, 30 mM sucrose, 0.7 μg/ml pepstatin, 4 mM pefabloc, 5 μg/ml leupeptin, 2 μg/ml aprotinin, and 7 mM sodium ortho-vanadate; all protease inhibitors from Boehringer), and were then centrifuged at 14,000 rpm at 4°C. The pellet was resuspended in cytoskeleton-stabilizing buffer plus 0.5% SDS. Protein concentration was determined using the Coomassie reagent (Pierce Chemical Co.), and 20 μg each of the supernatant and pellet were analyzed by SDS-PAGE and Western blot.

Immunoprecipitation and Western Blots

Whole-cell lysates were prepared by scraping adherent cultured cells into lysis buffer (1% Triton X-100, 1% deoxycholate in TBS, pH 7.5, with 10 mM EDTA, pH 8.0, 0.7 μg/ml pepstatin, 4 mM pefabloc, 5 μg/ml leupeptin, 2 μg/ml aprotinin, and 7 mM sodium ortho-vanadate). Tissue lysates were prepared the same way, except that they were dounce-homogenized in lysis buffer. The crude lysate was centrifuged at 14,000 rpm for 20 min in a microcentrifuge at 4°C to remove large particulates. The supernatant was passed through a 26 gauge needle to shear the DNA. Coomassie reagent (Pierce Chemical Co.) was used to determine the protein concentration of the cell and tissue lysates.

For coimmunoprecipitation studies, the above protocol was followed, and then primary antibody was added to the lysis supernatant and incubated for 1 h at 4°C, and precipitated by addition of Gamma-Bind Plus Sepharose beads (Amersham Pharmacia Biotech). The beads were washed five times with 1:10 diluted lysis buffer, and were then eluted by boiling in Laemmli sample buffer. Antibodies used for immunoprecipitating palladin were mAb C10 (for immunoprecipitations [IPs] from CEFs) and mAb 1E6 (for IPs from Swiss 3T3 cells). The antibody used for immunoprecipitating α-actinin was rabbit polyclonal A 2543 (Sigma-Aldrich).

For large-scale, preparative IPs of palladin (to obtain gel bands for microsequencing or immunization purposes), a clean precipitation was de-

[1]*Abbreviations used in this paper:* CEF, chick embryo fibroblast; EST, expressed sequence tag; IP, immunoprecipitation; MEF, mouse embryo fibroblast; pen/strep, 100 U/ml penicillin G, and 100 μg/ml streptomycin; RT-PCR, reverse transcriptase–PCR; VASP, vasodilator-stimulated phosphoprotein.

sired. In this case, best results were obtained if the actin cytoskeleton was first disassembled by trypsinizing the cells before lysis. Trypsinized cells were collected by centrifugation, the cell pellet was resuspended in the above lysis buffer on ice for 15 min, and then centrifuged and incubated with antibody, as described for coimmunoprecipitation studies.

For Western blot analysis, samples resolved on SDS-PAGE gels were transferred to either nitrocellulose (Fisher Scientific) or PVDF (NEN Life Science Products) membranes. Membranes were blocked in 5% nonfat dried milk in wash buffer (PBS with 0.5% Tween), and were then incubated with primary antibody for 1 h. After multiple changes of wash buffer, membranes were incubated with HRP-conjugated secondary antibody (Jackson Immunochemicals), and were then washed again before applying SuperSignal chemiluminescent substrate (Pierce Chemical Co.) and exposing to autoradiographic film (Eastman Kodak Co.). Purified α-actinin was the generous gift of Dr. Fred Pavalko (University of Indiana, Indianapolis, IN). Antiactin antibody was purchased from Chemicon; antivinculin (clone hVin-11), antitalin (8D4), and anti–α-actinin (A5044) were purchased from Sigma-Aldrich; antizyxin antibody was the gift of Dr. Mary Beckerle (University of Utah, Salt Lake City, UT).

Molecular Cloning of Palladin

Two cDNA libraries in λ phage (a day-10 chick embryo library and a day-11.5 mouse embryo library from CLONTECH Laboratories, Inc.) were plated at 50,000 plaque-forming units (pfu) per 150-mm plate; duplicate phage lifts were obtained using nitrocellulose membranes (Fisher Scientific) previously saturated in 10 mM isopropyl-β-D-thiogalactopyranoside (Sigma-Aldrich). 1,000,000 plaques of each library were screened using our pooled mAbs. Bound antibodies were detected using an alkaline phosphatase-conjugated secondary antibody (Jackson Immunochemicals) and nitroblue tetrazolium chloride–5-bromo-4-chloro-3-indolyl phosphate (Pierce Chemical Co.) as the colorimetric substrate. Positive plaques were picked, replated, and rescreened. Plaques that survived three rounds of screening were purified and the insert was obtained by PCR with λ primers (gt11 from Stratagene), using Pfu polymerase (Stratagene). The PCR product was blunt-end cloned into pBluescript and sequenced on both strands. Two partial, overlapping clones were found: a chick clone (18b-1; 884 bp; GenBank/EMBL/DDBJ accession #AF205077) and a mouse clone (7a-1; 1,580 bp; GenBank/EMBL/DDBJ accession #AF205078; see Fig. 3 A). The 7a-1 clone contained a stop codon near the 3′ end, followed by 100-bp of 3′ untranslated sequence. Neither 7a-1 nor 18b-1 contained a start codon. A thorough search of the nonredundant database using BLAST revealed several mouse and human expressed sequence tags (ESTs), only one of which had a 5′ extension (EST #AA671190 from 13.5-d mouse embryo heart). Based on the 5′ sequence of this EST and 5′ end of our 7a-1 mouse clone, we designed primers for reverse transcriptase–PCR (RT-PCR; 5′GAACTACAGAACACAGCAGCCTCCGAGG3′ as forward primer and 5′GTCCTCCTTGAAGCGAAGCTTCCGTTCC3′ as reverse primer). Poly A^+ RNA was prepared from 13.5-d mouse embryo hearts (see below) and used to make cDNA with Superscript II (GIBCO BRL). This cDNA was used as template for PCR with our primers, using Hi Fidelity Platinum Taq polymerase (GIBCO BRL). The resulting 1,433-bp PCR product (GenBank/EMBL/DDBJ accession #AF205079) was cloned into pBluescript and sequenced on both strands. A methionine with a Kozak sequence was located in this sequence, which was predicted to yield a protein of 85.7 kD. The full-length construct was made by piecing the two partial sequences together at their shared HindIII site. The myc-tagged full-length construct was made by PCR-cloning the entire open reading frame into the SmaI site of the pRK-MYC vector, downstream of, and in frame with, the myc tag.

Northern Blot Analysis

Total RNA was obtained by the Trizol method (GIBCO BRL). Poly A selection was done according to the method of Celano et al. (1993) using oligo-dT cellulose (GIBCO BRL). 5 μg of poly-A^+ RNA from different chick tissues was resolved on a formaldehyde gel and transferred to Duralon Nylon membrane (Stratagene) by capillary transfer. The RNA was then cross-linked to the membrane in a GS Gene Linker UV oven (Bio-Rad) using program C3 for damp membranes. Prehybridization was done in Quik-hyb buffer (Stratagene) and 100 μg/ml boiled salmon sperm DNA (GIBCO BRL) at 68°C. The chick cDNA (18b-1) was amplified by PCR from the pBluescript construct and labeled using DECAprime II DNA labeling kit (Ambion). This probe was then added to the membrane and hybridization was done at 68°C for 20 h. The membrane was washed twice for 30 min in 1× SSC/0.5% SDS at room temperature and twice for 30 min in 0.1× SSC/0.1% SDS at 65°C. The membrane was exposed to autoradiographic film (Eastman Kodak Co.) at −80°C overnight.

Transfection and Infection of Cells with Antisense Construct

The partial mouse cDNA, 7a-1, was cloned in the antisense orientation into the EcoRI site of the adenovirus shuttle vector, pAdlox. This construct was used in transient transfections, along with a GFP vector (pEGFP-N2 from CLONTECH Laboratories, Inc.) as a transfection marker. For infecting cells, the partial antisense construct in pAdlox was packaged into viral particles by the Cre-lox recombination method of Hardy et al. (1997). Three control viruses were also made. Empty viral particles were generated using pAdlox without an insert, and GFP-expressing virus was made using a pAdlox-EGFP construct. The third control virus expressed a mutant form of cdc42 that has been shown to be inactive (Bourne et al., 1991; Ridley et al., 1992). This virus was made by cloning A35-cdc42 (cdc42 with a Thr→Ala mutation at position 35) into pAdlox and was a kind gift of Sean Aeder and Dr. Ann Sutherland (University of Virginia, Charlottesville, VA). We confirmed the presence of the correct construct by restriction digest and sequencing of DNA from all recombinant viruses. Desalting of the viral preps was done using PD-10 columns prepacked with Sephadex™ G-25M (Amersham Pharmacia Biotech). Viral stocks were titered using transformed human embryonic kidney cells (293 cells) in a plaque assay, according to previous protocols (Tollefson et al., 1999). In brief, cells were infected in duplicate using eight different dilutions of each viral stock, and were then fed with agar overlay medium. 7 d after infection, cells were fed with the agar overlay medium containing 0.1% Neutral red (GIBCO BRL); plaques were counted at 9 and 10 d after infection.

Rcho-1 cells were transfected using lipofectamine PLUS reagent (GIBCO BRL) in growth medium without FBS and pen/strep. After 5 h, FBS and pen/strep were added. 2 d after transfection, the cells were induced to differentiate and monitored for 3 d (5 d after transfection).

MEFs were infected with recombinant virus as follows: the cells were incubated with the indicated concentration of each virus in half the usual volume of complete media. After 1 h, the media volume was brought up to the usual amount and the cells were left overnight. The next day, the infection medium was removed and fresh medium was added. Cells were followed for 3 d after infection.

Results

The C10 mAb Recognizes a Novel Protein that Colocalizes with α-Actinin

An mAb designated C10 was made over a decade ago by immunizing mice with partially purified vinculin and screening the hybridoma supernatants by immunofluorescent labeling of fibroblasts. At that time, C10 was misidentified as an anti–α-actinin antibody. Upon further characterization, we realized that C10 recognizes an antigen distinct from α-actinin, although the C10 antigen colocalized closely with α-actinin in many types of cells. As shown in Fig. 1 A, C10 stained regularly spaced puncta along actin stress fibers, and also stained the ends of the stress fibers intensely, a pattern that closely resembles the labeling that is typical of α-actinin. Like α-actinin, the C10 antigen also localized to the cell–cell junctions of epithelial cells (Fig. 1 C) and the Z-lines of embryonic cardiac myocytes (Fig. 1 D). When fibroblasts were double-labeled with C10 and a polyclonal antibody to α-actinin, the staining patterns were remarkably similar, as shown in Fig. 2. Both the C10 antibody (Fig. 2, A and D, in green) and the α-actinin antibody (Fig. 2, C and F, in red) strongly labeled the ends of actin stress fibers, and both antibodies also stained many of the same stress fiber puncta.

The C10 antibody did not perform well in immunoblots;

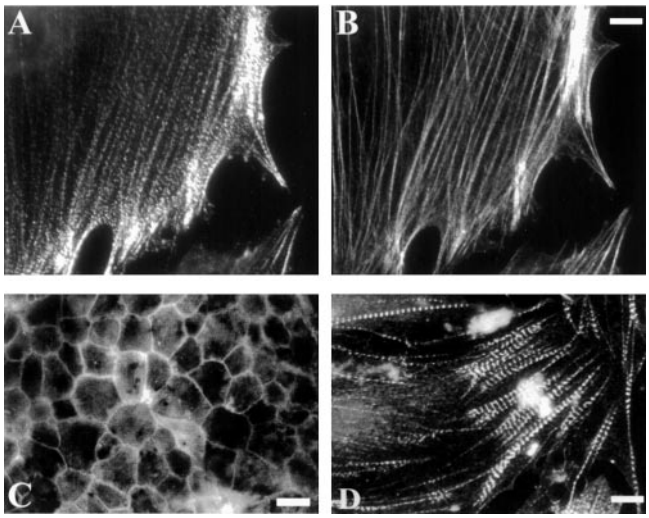

Figure 1. Immunofluorescent labeling with the C10 mAb. Cells were immunolabeled with C10 (A, C, and D) or fluorescent phalloidin (B). A and B, Cultured CEFs. C, Chick pigmented epithelium, in an en face preparation on gelatin-coated coverslips. D, Embryonic cardiac myocytes isolated from a day-10 chick heart. Bars: (B) 8 μm; (C) 20 μm; (D) 25 μm.

however, it did recognize native protein in detergent lysates of cultured chick fibroblasts. In IPs from ^{35}S-labeled, trypsinized CEFs, the major band resolved as a blurry doublet with an apparent molecular weight of 90–92 kD (Fig. 3 A), which is significantly smaller than the monomer molecular mass of α-actinin at 105 kD. This provided the first clue that the C10 antigen was distinct from α-actinin. The 90–92-kD band immunoprecipitated from CEFs was excised from Coomassie blue-stained gels and subjected to tryptic digestion, and a search of the GenBank/EMBL/DDBJ database revealed the tryptic map to be novel. Subsequently, three of the tryptic peptides, 9–15 residues in length, were sequenced by mass spectrometry, and analysis of the existing database showed that all three were novel (data not shown), thus providing additional evidence that the C10 antigen was a novel protein with no overall sequence similarity to α-actinin.

Not only did the C10 antibody fail to perform in Western blots, it also did not cross-react with species other than chicken, which severely limited its usefulness as a probe. To obtain better antibodies to the same antigen, the major band immunoprecipitated by the C10 mAb was excised from gels and used to immunize mice. mAbs were subsequently obtained and characterized: eight of these performed well in Western blots, and six of those blotting antibodies cross-reacted with all vertebrate species tested (including frog, mouse, rat, dog, and human). All mAbs recognized the same size protein in CEF lysate as the original C10 antibody. Furthermore, they also cross-reacted only with the protein precipitated by the C10 mAb on Western blot and not with purified α-actinin (Fig. 3 B).

The mAbs were used in Western blots to characterize the association of the C10 antigen with the actin cytoskeleton. To determine if the C10 antigen was tightly bound to the cytoskeleton, Triton extraction experiments were performed. MEFs were extracted in 0.5% Triton in a cytoskeleton stabilizing buffer (see Materials and Methods) and equal amounts of protein from the pellet and the supernatant were analyzed for palladin by Western blot. As shown in Fig. 3 C, most of the C10 antigen was found to be in the Triton-insoluble pellet, with only a small fraction in the soluble pool, indicating that the C10 antigen is tightly associated with the actin cytoskeleton.

The colocalization of the C10 antigen with α-actinin suggested that the two proteins might form a stable complex in vivo. To address this question, we immunoprecipitated the C10 antigen from adherent Swiss 3T3 cells and blotted for α-actinin. Fig. 3 D shows that α-actinin coimmunoprecipitates specifically with the C10 antigen (C10 IP lane) and not with Sepharose beads alone (preclear lane). This association depends on an intact cytoskeleton, because if the cells are first trypsinized, then lysed and immunoprecipitated for the C10 antigen, α-actinin does not coimmunoprecipitate (data not shown). The interaction appears to be specific, as only a trace amount of actin was detected in both the preclear lane and the IP lane (data not shown),

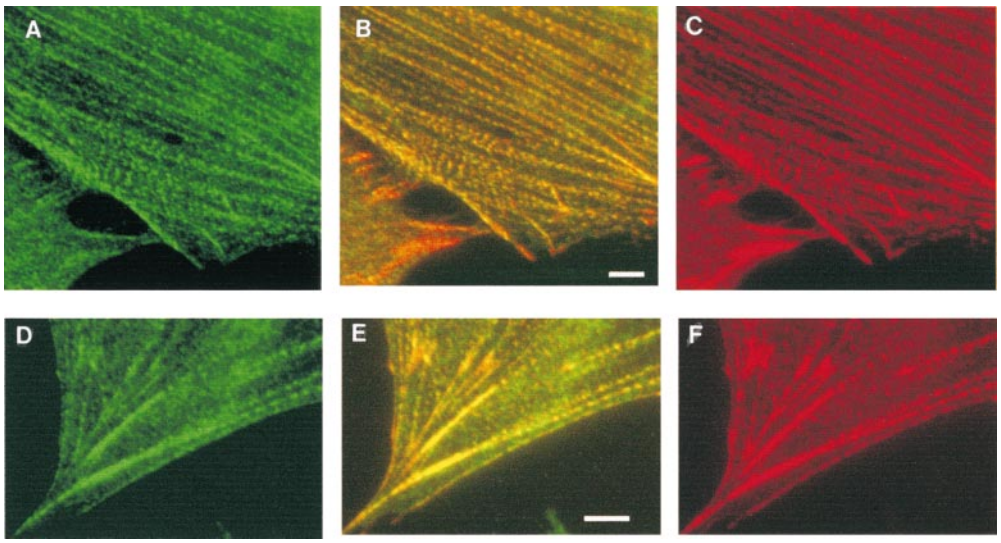

Figure 2. Colocalization of the C10 antigen and α-actinin in stress fibers. Cultured fibroblasts were stained with C10 mAb (A and D, green fluorescence) or polyclonal anti–α-actinin (C and F, red fluorescence). The merged images (B and E) show that the C10 antigen largely colocalizes with α-actinin in a punctate pattern along stress fibers and in a concentration at the ends of stress fibers. Bars, 5 μm.

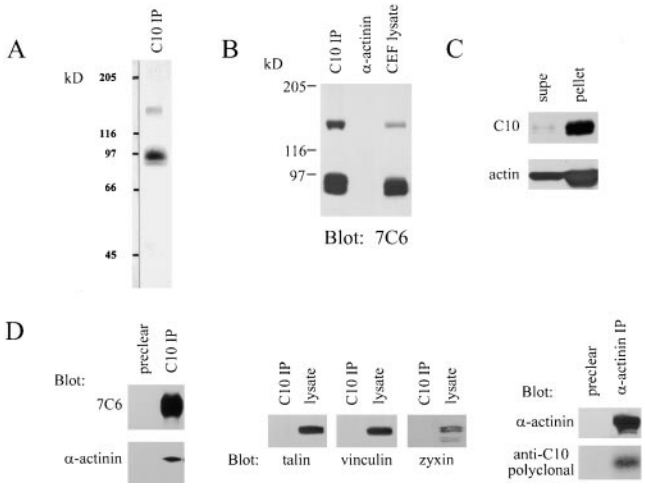

Figure 3. The C10 mAb immunoprecipitates a cytoskeleton-associated protein in lysates of fibroblasts. A, Immunoprecipitation from ^{35}S-labeled CEFs. Metabolically labeled fibroblasts were trypsinized and lysed on ice, and were then centrifuged. The supernatant was subjected to IP with the C10 mAb. The major band resolves as a broad doublet at 90–92 kD. B, The C10 antibody does not cross-react with α-actinin. C10 immunoprecipitates, purified α-actinin, and whole-cell lysate from cultured CEFs were resolved by SDS-PAGE and blotted with the anti-C10 mAb, 7C6. Note that 7C6 failed to detect purified α-actinin in the middle lane. C, Analysis of the fractionation of the C10 antigen. MEF lysates were extracted with 0.5% Triton X-100 in cytoskeleton-stabilizing buffer (see Materials and Methods) and the insoluble pellet was collected by centrifugation at 14,000 rpm. 20 μg of protein from pellets and supernatants was loaded and blotted with mAb 7C6. D, C10 antigen coimmunoprecipitates with α-actinin. 3T3 cells were scraped in lysis buffer on ice, the supernatant was precleared with Gamma-bind beads alone, and mAb 1E6 was conjugated to Gamma-bind beads, and was then used to immunoprecipitate the C10 antigen. Both sets of beads were eluted and blotted with either mAb 7C6 or anti–α-actinin mAb (left). To demonstrate the specificity of the coimunoprecipitation, the IPs were also blotted for talin, vinculin, and zyxin (all negative; center). In the reverse experiment, α-actinin was immunoprecipitated using a rabbit polyclonal antibody, and the IP was blotted for α-actinin and for the C10 antigen (right).

and the immunoprecipitates did not contain talin, vinculin, or zyxin as determined by Western blot (Fig. 3 D). The C10 antigen was also detected in α-actinin immunoprecipitates (Fig. 3 D), which adds further support to the idea that these two proteins are found in a complex in vivo. The relative intensity of the C10 and α-actinin band suggests that they do not coimmunoprecipitate in a 1:1 ratio, so that further experimentation will be required to determine if these two proteins bind directly to each other or if another unknown molecule contributes to the formation of an α-actinin–C10 antigen complex.

The blurred appearance of the C10 band in both IPs and Western blots suggested that the C10 antigen might be subject to posttranslational modification. As a first step towards identifying these modifications, the IPs were repeated using ^{32}P-labeled cells. Significant phosphorylation of the C10 antigen was detected, and phosphoamino acid analysis revealed that the C10 antigen is phosphorylated predominantly on serine residues and, to a lesser extent, on tyrosine residues (data not shown).

Molecular Cloning and Characterization of Palladin cDNA

The mAbs were pooled and used to screen both chick and mouse embryo cDNA libraries. Partial overlapping clones were obtained, which encoded the COOH-terminal two-thirds of the open reading frame, including the stop codon and 100 bp of the 3′ untranslated region (Fig. 4 A). Rescreening of the respective libraries with these partial clones as probes did not yield longer cDNAs. Using the sequence of the partial clones, we searched the EST database and found several matching sequences, most of which were also partial COOH-terminal fragments. One EST, a 3-kb long mouse embryo heart cDNA (GenBank/EMBL/DDBJ accession #AA671190), spanned our clones and extended them at the 5′ end. Using the partial sequence of this EST, we designed primers and performed RT-PCR using mouse embryo heart RNA. The 1,433-bp PCR product was sequenced, and a methionine with a Kozak consensus sequence (Kozak, 1991) was found near its 5′ end. With this methionine as the start site, the predicted molecular weight of the full-length clone would be 85.7 kD, close to the 90-kD molecular weight that had been estimated for the C10 antigen based on SDS-PAGE. To confirm that this was indeed the sequence of the 90-kD protein, we repeated the RT-PCR using RNA from Swiss 3T3 fibroblasts. The PCR product was sequenced and found to be identical to that obtained from mouse embryo heart.

The full-length clone (Fig. 4 D) contained all three of the tryptic peptides that had been obtained by microsequencing, increasing our confidence that we had successfully cloned the C10 antigen. The partial chick clone, 18b-1, was found to be 72% identical to the mouse clone over that region of the protein (amino acids 61–330, data not shown). To further verify that we had cloned the correct cDNA, we expressed the full-length clone with an epitope tag. The myc-tagged construct was transfected into Swiss 3T3 fibroblasts and stained with an antimyc antibody. As shown in Fig. 4 B, the myc-tagged construct localized in precisely the same striated pattern that had been observed for the endogenous C10 antigen. By Western blot, both antimyc antibodies and anti-C10 monoclonals detected the same band (Fig. 4 B). Together, these results confirm that we have succeeded in cloning the same protein that was detected by the original C10 antibody and this novel protein was named palladin.

Analysis of Protein Motifs in Palladin

The sequence of the full-length clone was analyzed by BLAST search of the nonredundant GenBank/EMBL/DDBJ database to identify proteins with homology to palladin, and by SMART search (Schultz et al., 1998) to identify conserved domains. The results of this analysis are summarized diagrammatically in Fig. 4 C. In the NH_2-terminal half of palladin, a proline-rich region was observed (amino acids 99–289, 30% proline overall). This region contains three polyproline motifs (FPPPP, LPPPPP, and SPPPPP, underlined in Fig. 4 D) homologous to those contained in zyxin, vinculin, and VASP/Mena family mem-

A

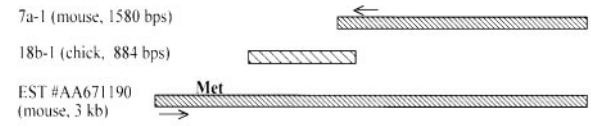

B

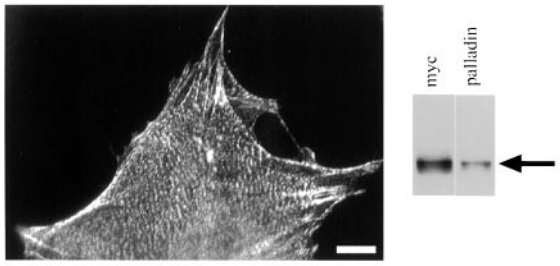

C

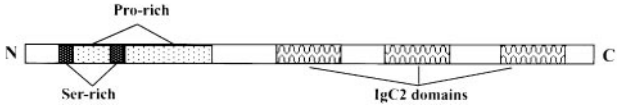

D

```
1    MAALQMQFNTAERETNGVHPSHGVNGLINGKAYGNKSPPT   40

41   PTALLSPTKEPPPLLAKPKLDPLKLQQLQNQVRLEQEACA   80

81   WPPAPPGVPCNSSSSGSSAPPSPPFPPPPPAFPELAACAS   120
                  *******
121  PVPSEPMSALASRATAMQSSGSFNYARPKQFIAAQNLGPA   160

161  SGLPTPTSSPSSSSLPSPLSPTPRPFGRAPGPPFVEPEAM   200
               *******
201  WGPSSPSPPPPPPPVFSPSAAYPVPDVFPLPPPPPPLPSS   240

241  TSHCASPARFGPGQTPAAFLSALLPSQPPPVAVNALGLPK   280

281  GVTPPGFPKKSSRTARIASDEEIQGTKDAVIQDLERKLRF   320

321  KEDLLNNGQPRLTYEERMARRLLGADSANVFNIQEPEETA   360

361  ANQEYKVSSCEQRLISEIEYRLERSPVDESGDEVQDPDVP   400

401  VENATAPFFEMKLKHYKIFEGMPVTFTCRVAGNPKPKIYW   440
                              ^^^^^^^^^^^^^^^^^^^^^^^^
441  FKDGKQISPKSDHYTIQRDLDGTCSLHTTASTLDDDGNYT   480
     ^^^^^^^^^^^^^^^^^^^^^^^^^^^^^^^^^^^^^^^^^^^^^^^^
481  IMAANPQGRVSCTGRLMVQAVNQRGRSPRSPSGHPHARRP   520
     ^^^^^^^^
521  RSRSRDSGDENEPIQERFFRPHFLQAPGDLTVQEGKLCRM   560
                                        ^^^^^^^^
561  DCKVSGLPTPDLSWQLDGKPIRPDSAHKMLVRENGVHSLI   600
     ^^^^^^^^^^^^^^^^^^^^^^^^^^^^^^^^^^^^^^^^^^^^^^^^
601  IEPVTSRDAGIYTCIATNRAGQNSFNLELVVAAKEAHKAP   640
     ^^^^^^^^^^^^^^^^^^^^^^^
641  VFMEKLQNTGVADGYPVRLECRVSGVPPPQIFWKKENESL   680
                  ^^^^^^^^^^^^^^^^^^^^^^^^^^^^^^^^
681  THSTERVSMHQDNHGYICLLIQGATKEDAGWYTVSAKNEA   720
     ^^^^^^^^^^^^^^^^^^^^^^^^^^^^^^^^^^^^^^^^^^^^^^^^
721  GIVSCTARLDVYTQWHQQPQTTKPKKVRPSASRYAALSDQ   760
     ^
761  GLDIKAAFQPEASPSHLTLNSGLVESEDL&             789
```

Figure 4. Molecular cloning and characterization of the C10 antigen. A, The pooled mAbs recognized a clone (7a-1) from an 11.5-d mouse embryo library and also a clone (18b-1) from a 10-d chick embryo library. A thorough BLAST search of the EST database identified a 3-kb EST from mouse embryo heart. The indicated primers (based on 7a-1 and the mouse EST) were used to perform RT-PCR on mouse mRNA. The start methionine with the Kozak sequence is shown. B, The full-length clone localizes properly and is recognized by anti-C10 antibodies. The myc-tagged construct was transfected into Swiss 3T3 cells, which were fixed and stained with an antimyc antibody. Note that the construct localized in focal adhesions, at the ends of stress fibers, and in a punctate pattern along the stress fibers. The transfected cells were also lysed and analyzed by Western blot. The same band is recognized by both antimyc and anti-C10 mAb 7C6. Bar, 10 μm. C, Cartoon of palladin protein. Domains identified using various programs, including proline-rich and serine-rich regions, are indicated. D, Protein sequence of palladin. Serine-rich areas are indicated with asterisks (*). Proline-rich motifs homologous to zyxin and VASP/Mena family members are underlined. The three tryptic peptides are indicated in bold-type, and the three IgC2 domains are indicated with carets (^). The stop codon is indicated by the ampersand (&).

bers. The proline-rich sequences are flanked by numerous serine residues. Also of interest are the three tandem repeats of an Ig-like sequence called the Ig C2 domain. Ig C2 domains have been identified previously in a group of intracellular proteins that are associated with the actin cytoskeleton in skeletal muscle, including the giant protein, titin (Labeit et al., 1990); the muscle-specific C protein (Einheber and Fischman, 1990), H protein (Vaughan et al., 1993), and M protein (Noguchi et al., 1992); myosin light chain kinase (Olson et al., 1990); and myotilin (Salmikangas et al., 1999). The Ig C2 domains in palladin share varying degrees of homology with previously identified proteins. The most NH_2-terminal Ig C2 domain of palladin has the highest homology to the NH_2-terminal, Z-line-associated, Ig C2 domains of titin (44% at the protein level), and the COOH-terminal Ig C2 domains of myosin light chain kinase (42%). Palladin's middle and COOH-terminal Ig C2 domains are most homologous to myotilin's NH_2-terminal Ig C2 (60% and 55%, respectively) and titin's COOH-terminal, M-line–associated, Ig C2 domains (48% and 37%, respectively).

Palladin Exists as Multiple Isoforms and Is Widely Expressed in Embryonic Tissues

Northern blot analysis of three tissues (brain, heart, and gizzard) from a day-10 embryonic chick were probed with the chick cDNA, 18b-1. As shown in Fig. 5 A, the major band in all three tissues was 4.4 kb. In addition, a larger transcript (6 kb) was detected in brain and gizzard, and faintly detected in heart. The largest band seen by Northern blot was a transcript of 7.4 kb, which was only observed in heart. The existence of multiple isoforms of palladin was confirmed by Western blot. As shown in Fig. 5 A, the protein bands detected by antipalladin mAb 1E6 corresponded precisely to the sizes that were predicted from the mRNA transcripts seen in the Northern blot. A doublet of 90–92 kD was detected in all three chick tissues. In brain and gizzard, a less intense band of 140 kD was stained, and a band of 200 kd was observed specifically in heart. An unusual band of 99 kD was also detected specifically in the Western blot of heart (Fig. 5 A). A corresponding size of message was not detected in the Northern blot, suggesting that the 99-kD band may result from post-translational modification of the 92-kD isoform.

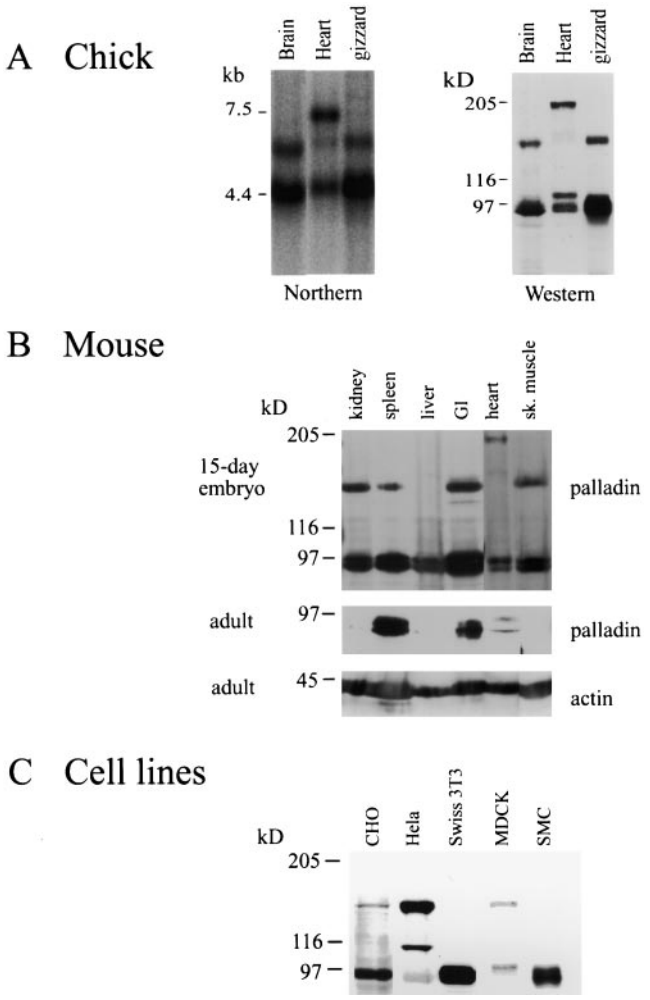

Figure 5. A, Palladin exists as multiple size variants. Left, Northern blot of poly-A^+ RNA isolated from brain, heart, or gizzard of a day-10 chick embryo and probed under high-stringency conditions using the chick clone 18b-1 as probe. Right, Western blot of protein extracted from the same tissues, blotted using anti-C10 mAb 1E6. For every size of palladin mRNA detected in the Northern blot, a corresponding size of protein was identified. B, Palladin expression is developmentally regulated in certain tissues. Embryonic and adult mouse tissues were extracted as described in Materials and Methods. 30 μg of protein was loaded in each lane and blotted with antipalladin mAb 7C6 or an mAb to actin. Note that palladin expression is ubiquitous in the embryo and restricted to a small number of tissues in the adult. C, Palladin isoforms are detected in cultured cells. Whole cell lysates were prepared as described in Materials and Methods. 30 μg of protein was loaded in each lane and blotted with antipalladin mAb 7C6.

To compare the pattern of palladin expression in embryonic versus adult tissues, immunoblot analysis was performed on six tissues obtained either from a day-15 mouse embryo or from an adult mouse. As shown in Fig. 5 B, the 90–92-kD form of palladin was detected in all embryonic tissues tested. The larger 140-kD isoform was present in embryonic kidney, spleen, gut, and skeletal muscle, but not in liver or heart. Embryonic mouse heart also expressed the 200-kD isoform. In the adult tissues, however, the expression of palladin was more variable (Fig. 5 B). Only the 90–92-kD isoform was detected and only in adult spleen and gut; it was almost undetectable in adult kidney, liver, heart, and skeletal muscle.

Palladin Isoforms Are Expressed in Cultured Cells

Since organized tissues contain a variety of cell types, we used cultured cell lines to determine if the palladin size variants seen in developing tissues could be assigned to specific types of cells. Palladin expression was compared in primary cultures of fibroblasts and vascular smooth muscle cells, as well as in the epithelial cell lines MDCK, CHO, and HeLa. As shown in Fig. 5 C, the 90–92-kD isoform of palladin was detected in Swiss 3T3 fibroblasts and in smooth muscle cells, which have a fibroblast-like morphology in culture; a faint band at 140 kd was sometimes detected in fibroblasts (see Fig. 3 A). However, all epithelial cells tested expressed both the 90–92-kD and the 140-kD isoforms, and an additional band of 110 kD was detected in HeLa cells. While preliminary, these results suggest the possibility that the 90–92-kD and 140-kD forms of palladin may be specifically associated with fibroblast-type and epithelial-type cytoarchitecture, respectively.

Palladin Expression Correlates with Cytoskeletal Organization in Differentiating Trophoblasts

The ubiquitous presence of palladin in developing tissues suggests that this protein may have a special role in organizing the actin cytoskeleton in cells that are undergoing the process of structural and functional differentiation. To investigate the function of palladin in cultured cells, we sought a cell line that undergoes cytoskeletal reorganization in response to specific growth conditions. We chose the rat choriocarcinoma (Rcho-1) cell line, which has been used as an in vitro model for rodent trophoblast giant cell differentiation (Faria and Soares, 1991). These cells grow as proliferative stem cells in medium containing 20% FBS, and the stem cells have a generally round morphology (Kamei et al., 1997). As shown in Fig. 6 A, top, the Rcho-1 stem cells have a poorly organized cytoskeleton: actin is localized in rings or patches, and no stress fibers are visible. Rcho-1 stem cells also have only small, peripheral focal complexes (Fig. 6 A, top).

Rcho-1 cells can be induced to differentiate into trophoblast giant cells by switching the medium from 20% FBS to 10% horse serum for three to seven days. Upon differentiation, Rcho-1 cells undergo a dramatic change in morphology and cytoskeletal organization (Fig. 6 A, bottom): the cells form abundant stress fibers and large, numerous focal adhesions. Western blot analyses were performed on Rcho-1 cells to determine if proteins associated with stress fibers and focal adhesions were upregulated in differentiated cells. As shown in Fig. 6 B, the expression of actin, α-actinin, and vinculin did not change in Rcho-1 stem cells versus differentiated cells; however, palladin expression was undetectable in the stem cell population, and increased dramatically by three to seven days after differentiation (Fig. 6 C). This correlation suggested that palladin could play an important role in cytoskeletal organization and remodeling in this cell model. It should

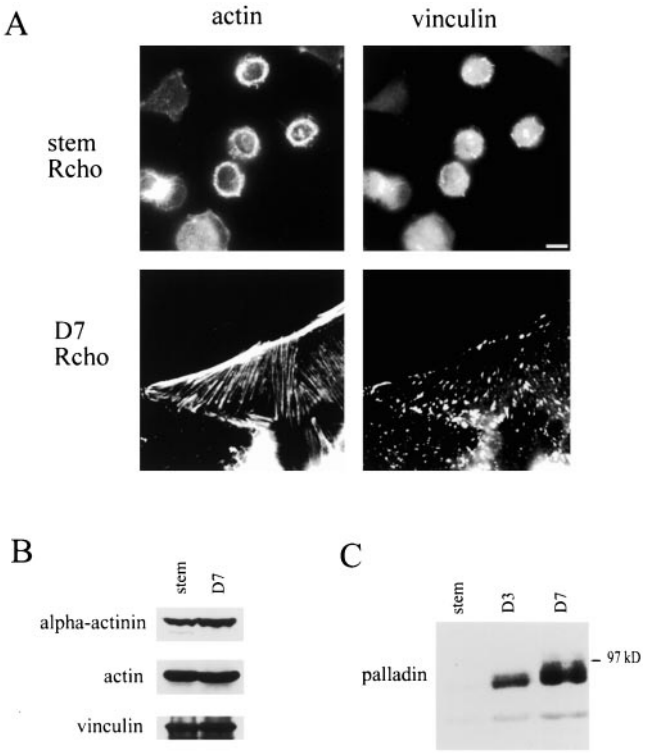

Figure 6. Rcho-1 cells upregulate the expression of palladin, concomitant with the formation of stress fibers and focal adhesions. A, Proliferative Rcho-1 stem cells have no organized actin stress fibers; when induced to differentiate, the cells assemble numerous stress fibers and large focal adhesions. Bar, 10 μm. B, Expression of actin, α-actinin, and vinculin does not change when Rcho-1 cells differentiate. Whole cell lysates were prepared by scraping cells in boiling Laemmli sample buffer; equal amounts of lysates were loaded in each lane and blotted for the respective protein. C, Palladin expression increases in differentiating cells. Whole cell lysates were prepared as in B and equal amounts loaded in each lane and blotted with antipalladin mAb 7C6. Only the 90–92-kD isoform was detected. D3 and D7 refer to 3 and 7 d after differentiation.

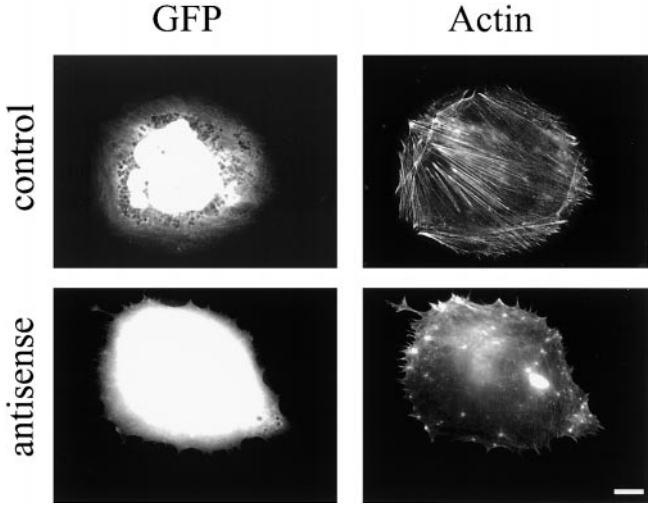

Figure 7. Rcho-1 cells fail to make stress fibers when treated with palladin antisense. A GFP vector was cotransfected either with an empty pAdlox vector (top) or with pAdlox–palladin antisense construct (bottom) into Rcho-1 stem cells. 2-d later, the cells were induced to differentiate. Three days after differentiation, the cells were fixed and stained with Texas red-conjugated phalloidin. Representative transfected cells are shown. Note that in the presence of the antisense construct, the cells have no stress fibers. Bar, 10 μm.

be noted that Rcho-1 cells express only the 90–92-kD form of palladin.

The role of palladin in Rcho-1 cells was explored further by using antisense technology. A partial antisense construct, corresponding to the COOH-terminal two-thirds of palladin, was made in the adenoviral vector, pAdlox. This construct was cotransfected with a GFP construct (as a transfection marker) into Rcho-1 stem cells. Control transfections were performed using both the empty pAdlox vector and the GFP construct. Two days after transfection, the cells were induced to differentiate by switching the medium from 20% FBS to 10% horse serum. After three days of differentiation, the cells were fixed and analyzed, since most cells lost expression of the GFP marker at later times. The cells were stained with phalloidin and all GFP-positive cells were scored for the presence of stress fibers. These experiments revealed that only 17% of the control-transfected cells (n = 120) lacked stress fibers, whereas 53% of the antisense-transfected cells (n = 132) failed to form stress fibers in response to the change in serum concentration. Representative examples of control-transfected and antisense-transfected cells stained with phalloidin are shown in Fig. 7. These results support the conclusion that expression of palladin is important for the formation of stress fibers in Rcho-1 trophoblast cells. Because Rcho-1 cells are not widely known, we decided to extend the antisense approach to investigate the role of palladin in a more commonly used cell type, cultured fibroblasts.

Palladin Antisense Treatment Alters the Cytoskeleton and Causes Cell Rounding in Fibroblasts

In initial antisense experiments on fibroblasts, both Swiss 3T3 cells and primary MEFs were transfected with the same antisense construct described above, and the effect on the actin cytoskeleton was monitored at three days after transfection by staining with rhodamine phalloidin. In both types of fibroblasts, a loss of stress fibers was observed (data not shown); however, the transfection efficiency was much lower than in Rcho-1 cells (<10% in fibroblasts, as compared with 30% in Rcho-1), resulting in a small sample of antisense-transfected cells. To obtain larger populations of antisense-treated cells, we decided to make a recombinant adenovirus to deliver the palladin antisense construct. Four viruses were made: one expressing the partial palladin antisense; one expressing no construct, to use as a control; and two containing irrelevant inserts (GFP and inactive cdc42) as additional specificity controls. MEFs were infected separately with equal concentrations of these four viruses, and the effect on palladin expression was analyzed by Western blot. As shown in Fig. 8 A, palla-

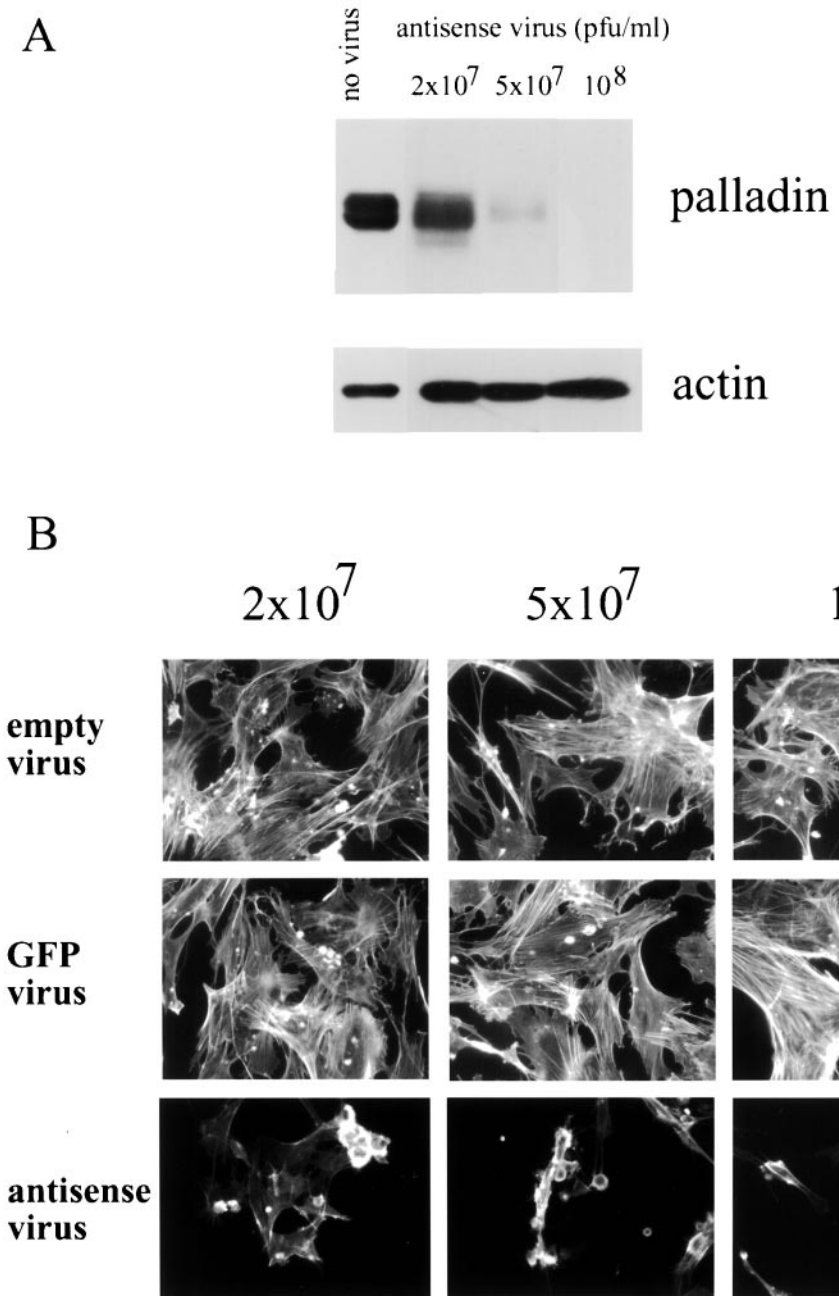

Figure 8. Reduced expression of palladin in MEFs results in a loss of stress fibers and focal adhesions. A, Adenovirus was used to deliver palladin antisense. Increasing concentrations of antisense virus leads to decreased palladin expression in MEFs. 3 d after infection, cell lysates were prepared by scraping cells in boiling Laemmli sample buffer. Blots were stained with antipalladin mAb 7C6 and antiactin (to check for equal loading). B, Increasing concentrations of antisense virus results in a loss of stress fibers and in cell rounding. MEFs were infected either with control adenovirus (empty virus or GFP-expressing virus) or with palladin antisense virus. 3 d after infection, cells were fixed and stained with Texas red-conjugated phalloidin. Bar, 20 μm.

din expression in the antisense-treated cells was dramatically decreased, and this decrease was specific, as it correlated with increasing concentrations of antisense virus. Empty virus and the two other control viruses did not significantly affect palladin expression (data not shown).

At three days after infection, phalloidin staining of infected cells was performed to assay the effect on the actin cytoskeleton. Cells infected with the empty virus remained well-spread and had numerous stress fibers (Fig. 8 B), as did cells infected with virus expressing GFP (Fig. 8 B) or inactive cdc42 (data not shown). In cells infected with increasing concentration of the antisense virus, an increasing proportion of the cells was observed to have assumed a rounded morphology (Fig. 8 B). At the highest concentration of virus, where >90% of the cells were infected (according to parallel infections with the GFP virus), virtually all cells were rounded.

The appearance of the actin cytoskeleton was also assayed in some cells at earlier times after antisense treatment. As shown in Fig. 9, the cells with a lowest level of palladin expression (as determined by immunofluorescent labeling) lacked robust stress fibers and instead had wispy arrays of actin (Fig. 9, B and D). In addition, cells with reduced palladin expression displayed focal adhesions only at the periphery and showed a striking absence of focal adhesions in the interior of the cell (Fig. 10, B and D). Taken together, these results suggest that the expression of palladin is required for cultured fibroblasts to maintain a normal organization of actin and focal adhesions.

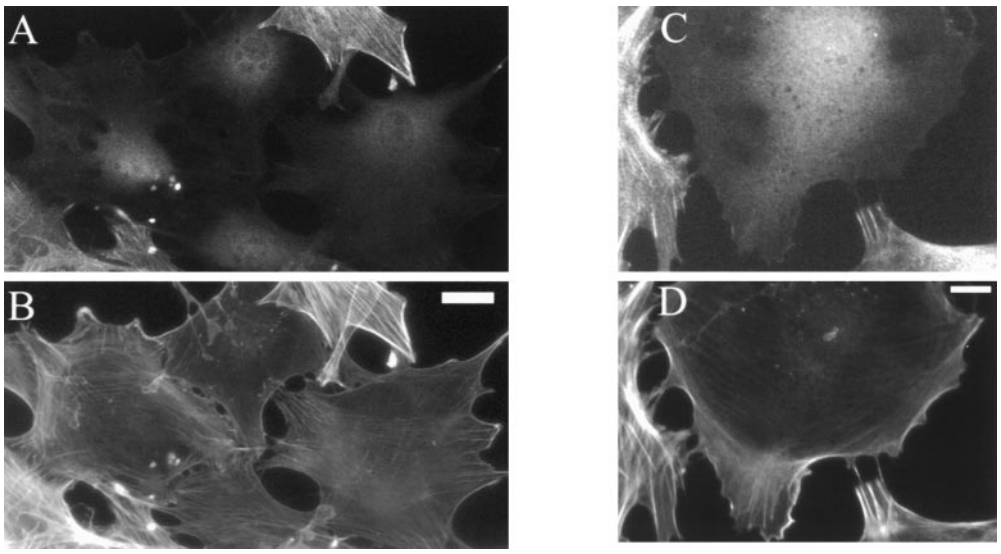

Figure 9. Loss of palladin expression results in a loss of stress fibers. At 2 d after infection, at the lowest virus concentration (2×10^7 pfu/ml), cells were fixed and stained with a 1:1 mixture of antipalladin mAbs 7C6 and 1E6 (A and C), and phalloidin (B and D). In each field examined, the cells with the lowest level of palladin staining exhibited a more round morphology and a lack of robust stress fibers. Bars: (A and C) 10 μm; (B and D) 5 μm.

Discussion

Here, we describe a novel protein that was found in an unusual way, by recognizing that an older mAb had been mischaracterized and by identifying the correct antigen. Palladin is a new member of a small group of cytoskeletal proteins that contain Ig C2. The Ig C2 repeat was first identified in the extracellular domain of cell surface molecules involved in cell adhesion (Williams and Barclay, 1988). Subsequently, the Ig C2 repeat was found in intracellular proteins, including the giant protein titin, which contains up to 166 copies of this motif (Labeit et al., 1990). Ig C2 domains are characteristic of many members of the myosin-binding superfamily, such as C protein, H protein, and M protein (Einheber and Fischman, 1990; Noguchi et al., 1992; Vaughan et al., 1993). The majority of the intracellular Ig C2 domain proteins are found specifically in striated muscle (Furst and Gautel, 1995), suggesting that Ig C2 domains may have a special role in achieving the highly ordered cytoskeletal structure of the sarcomere. It is somewhat surprising, then, that palladin has been detected in every embryonic tissue tested to date, and its expression is actually downregulated in striated muscle of mature animals.

The function of the Ig C2 domain has been widely debated. There appears to be the potential for functional specialization of the Ig C2 repeats found within a single molecule. In titin, for example, two Ig C2 repeats at the extreme NH_2-terminal end bind to a novel Z-line protein called the T-cap (Gregorio et al., 1998). In the C protein, a high-affinity binding site for myosin has been mapped specifically to the COOH-terminal Ig C2 domain, and this activity is not shared with the remaining six Ig C2 domains found in the same protein (Okagaki et al., 1993). The ability to bind myosin is not a universal feature of the intracellular Ig C2 domain proteins, as the Z-line protein myotilin does not appear to bind myosin; instead, the Ig C2 do-

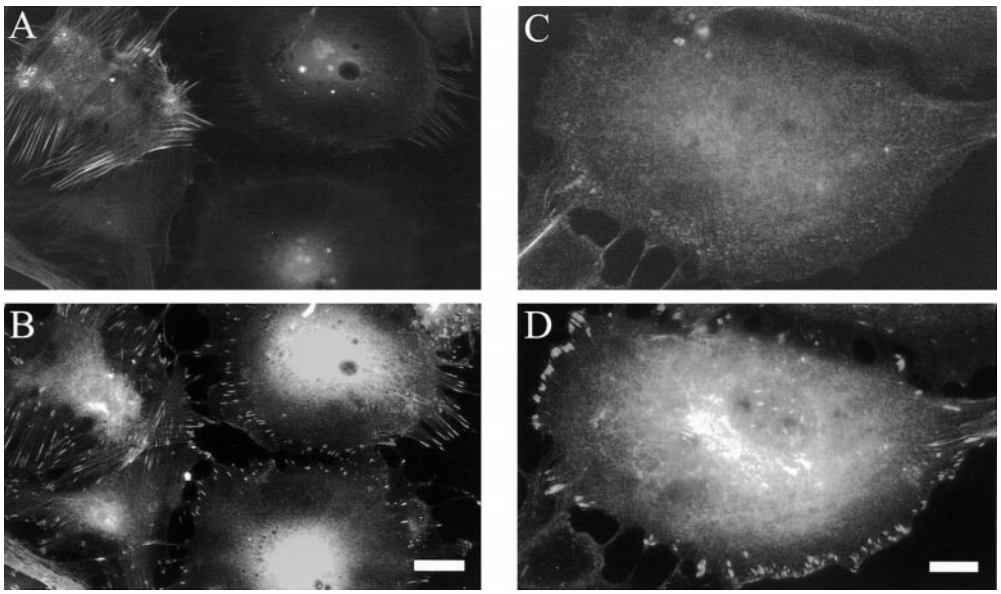

Figure 10. Cells with attenuated palladin expression have only peripheral focal adhesions. At 2 d after infection (as in Fig. 9), cells were fixed and stained for palladin with a 1:1 mixture of mAbs 7C6 and 1E6 (A and C) and double-labeled for paxillin (B and D), as a focal adhesion marker. Cells with the lowest level of palladin staining consistently exhibited a clearing of focal adhesions from the center of the cell, such that only peripheral focal adhesions remained. Bars: (A and C) 10 μm; (B and D) 5 μm.

mains of myotilin have been implicated in the formation of homodimers (Salmikangas et al., 1999). Additional experiments will be needed to determine the function of palladin's Ig C2 domains; however, careful sequence comparison has shown that the three Ig C2 domains of palladin are, overall, more highly homologous to those of myotilin and titin, rather than to those of C protein or M protein.

Another striking feature of palladin is the polyproline region in the NH_2-terminal half of the molecule. Proline-rich sequences have been shown to play an important role in the reorganization of the actin cytoskeleton, based on analysis of the *Listeria monocytogenes* protein, ActA. It is thought that the intracellular pathogen, *Listeria*, is able to usurp the host cell's cytoskeleton because the ActA protein mimics host cell proteins that normally regulate actin-based cell motility (Kocks et al., 1992). ActA contains four proline-rich repeats that have been shown to serve as docking sites for members of the Ena/VASP family of proteins (Smith et al., 1996; Niebuhr et al., 1997). A sequence within the proline-rich repeats, FPPPP, is minimally sufficient to bind the EVH1 domain of Ena/VASP family members in vitro (Niebuhr et al., 1997; Prehoda et al., 1999). This sequence has been found in two eukaryotic proteins, zyxin and vinculin (Reinhard et al., 1995b; Brindle et al., 1996; Gertler et al., 1996; Huttelmaier et al., 1998). Zyxin and vinculin may share limited functional homology with ActA: both proteins bind to VASP in vitro and both are concentrated in subcellular sites that are enriched in actin filaments. Zyxin is of particular interest, because it contains three FPPPP sequences and colocalizes with VASP, both in focal adhesions and along the stress fibers (Beckerle, 1998).

In addition to the FPPPP motif, a second polyproline sequence has been implicated in actin-based motility. The sequence XPPPPP (where X = A, G, L, or S) is shared between a group of actin regulatory proteins including zyxin, VASP, its *Drosophila* relative Ena, and the human Wiscott-Aldrich syndrome protein (Symons et al., 1996; Purich and Southwick, 1997; Zeile et al., 1998). In VASP, this sequence has been shown to bind to the G actin-binding protein, profilin (Reinhard et al., 1995a; Kang et al., 1997). While the precise role of the FPPPP and XPPPPP motifs in eukaryotic proteins is not yet clear, it is nevertheless intriguing that palladin contains copies of both consensus sequences, and thus shares limited homology with a group of molecules that have been implicated in modulating the assembly of actin filaments. Future experiments will focus on identifying the in vivo binding partners that interact with the polyproline sequences of palladin.

The existence of multiple size variants of palladin has been demonstrated by Northern and Western blot, and the pattern of isoform expression appears to be determined by both cell type and developmental status. This suggests the interesting possibility that certain isoforms of palladin may be adapted for participation in specialized cytoskeletal organizations. The 90–92-kD form, which is the one we have cloned and sequenced, is the most abundant and ubiquitous in tissues of both the embryonic and adult mouse. Whereas it appears that one or more isoforms of palladin are expressed in every tissue of a developing mouse or chick, palladin expression was greatly reduced in a number of adult tissues, including heart, skeletal muscle, liver, and kidney. One explanation for this pattern could be that palladin is involved in establishing the cytoskeletal organization of cells as they differentiate, and that palladin is then replaced by another protein in certain fully differentiated cells. For example, the palladin detected in embryonic muscle may be replaced in differentiated sarcomeres by the related molecule myotilin, which is specific to striated muscle (Salmikangas et al., 1999).

Although much remains to be learned about the regulation of palladin and its in vivo protein–protein interactions, two lines of evidence suggest that palladin plays a role in the organization of the actin cytoskeleton in cultured cells. First, in the Rcho-1 cell line, endogenous palladin expression is specifically upregulated when the cells began to assemble stress fibers and focal adhesions in response to a change in serum concentration. Although this result is only correlative, it is compelling to note that Rcho-1 stem cells, which do not assemble stress fibers, nonetheless express the same amount of actin as the differentiated cells that form abundant stress fibers. To date, the only cytoskeletal protein found to be upregulated in the differentiated Rcho-1 cells is palladin, suggesting that this protein may be key to the dramatic cytoskeletal reorganization observed in these cells. The second line of evidence was obtained by attenuating the expression of palladin with antisense constructs, introduced either by transfection or by delivery via adenovirus. Using either method, in primary fibroblasts, the result was the same: cells with low levels of palladin expression displayed few, wispy stress fibers and few, peripheral focal adhesions, and eventually rounded up from the substrate. Together, these data indicate that palladin is important for the maintenance of organized arrays of actin and associated cell adhesions. Future experiments will focus on understanding the mechanism by which palladin has this effect. It will be interesting to determine if palladin has its primary action on the assembly of actin microfilaments or, like α-actinin, on the bundling of microfilaments to form stable stress fibers, or on the anchorage of microfilaments to the focal adhesions.

We owe many thanks to Dr. Keith Burridge, in whose lab the C10 mAb was produced, and to Dr. Ann Sutherland for providing advice, mouse dissections, and temporary space. We thank members of the Otey lab for helpful discussions, Drs. Amy Bouton, Judy White, and Steve Gonias for valuable suggestions, Dr. Bill Sutherland for assistance with the production of mAbs, Dr. John Leszyk for peptide microsequencing, Sean Aeder and Dr. Dan Engel for help with the production of adenovirus, Drs. Olli Carpen and Olli-Matti Mykkanen for generously discussing unpublished results, and Dr. Richard Cheney and Jonathan Berg for help with imaging.

This work was supported by National Institutes of Health grants GM50974 to C. Otey, HD34807 to Ann Sutherland, and GM29860 to Keith Burridge.

Submitted: 1 December 1999
Revised: 15 June 2000
Accepted: 22 June 2000

References

Aberle, H., H. Schwartz, and R. Kemler. 1996. Cadherin–catenin complex: protein interactions and their implication for cadherin function. *J. Cell. Biochem.* 61:514–523.

Adams, C.L., W.J. Nelson, and S.J. Smith. 1996. Quantitative analysis of cadherin–catenin–actin reorganization during development of cell–cell adhesion. *J. Cell Biol.* 135:1899–1911.

Arber, S., G. Halder, and P. Caroni. 1994. Muscle LIM protein, a novel essential regulator of myogenesis, promotes myogenic differentiation. *Cell.* 79: 221–231.

Arber, S., J.J. Hunter, J. Ross, M. Hongo, G. Sansig, J. Borg, J.-C. Perriard, K.R. Chien, and P. Caroni. 1997. MLP-deficient mice exhibit a disruption of cardiac cytoarchitectural organization, dilated cardiomyopathy and heart failure. *Cell.* 88:393–403.

Beckerle, M. 1998. Spatial control of actin filament assembly: lessons from *Listeria*. *Cell.* 95:741–748.

Bourne, H.A., D.A. Sanders, and F. McCormick. 1991. The GTPase superfamily: conserved structure and molecular mechanism. *Nature.* 349:117–127.

Brindle, N.P., M.R. Holt, J.E. Davies, C.J. Price, and D.R. Critchley. 1996. The focal-adhesion vasodilator-stimulated phosphoprotein (VASP) binds to the proline-rich domain in vinculin. *Biochem. J.* 318:753–757.

Carpen, O., P. Pallai, D.E. Staunton, and T.A. Springer. 1992. Association of intercellular adhesion molecule (ICAM-1) with actin containing cytoskeleton and α-actinin. *J. Cell Biol.* 118:1223–1234.

Celano, P., P.M. Vertino, and R.A. Casero, Jr. 1993. Isolation of polyadenylated RNA from cultured cells and intact tissues. *Biotechniques.* 15:26–28.

Chang, J.H., W.M. Sutherland, and S.J. Parsons. 1995. Monoclonal antibodies to oncoproteins. *Methods Enzymol.* 254:430–445.

Christerson, L.B., C.A. Vanderbilt, and M.H. Cobb. 1999. MEKK1 interacts with alpha-actinin and localizes to stress fibers and focal adhesions. *Cell. Motil. Cytoskel.* 43:186–198.

Craig, S.W., and R.P. Johnson. 1996. Assembly of focal adhesions: progress, paradigms and portents. *Curr. Opin. Cell Biol.* 8:74–85.

Crawford, A.W., J.W. Michelsen, and M.C. Beckerle. 1992. An interaction between zyxin and α-actinin. *J. Cell Biol.* 116:1381–1393.

Dabiri, G.A., K.K. Turnacioglu, J.C. Ayoob, J.M. Sanger, and J.W. Sanger. 1999. Transfections of primary muscle cell cultures with plasmids coding for GFP linked to full length and truncated muscle proteins. *Methods Cell. Biol.* 58:239–260.

Djinovic-Carugo, K., P. Young, M. Gautel, and M. Saraste. 1999. Structure of the alpha-actinin rod: molecular basis for crosslinking of actin filaments. *Cell.* 98:537–546.

Einheber, S., and D.A. Fischman. 1990. Isolation and characterization of a cDNA clone encoding avian skeletal muscle C-protein: an intracellular member of the immunoglobulin superfamily. *Proc. Natl. Acad. Sci. USA.* 87: 2157–2161.

Faria, T.N., and M.J. Soares. 1991. Trophoblast cell differentiation: establishment, characterization and modulation of a rat trophoblast cell line expressing members of the placental prolactin family. *Endocrinology.* 129:2895–2906.

Faulkner, G., A. Pallavicini, E. Formentin, A. Comelli, C. Ievolella, S. Trevisan, G. Bortoletto, P. Scannapieco, M. Salamon, V. Mouly, et al. 1999. ZASP: a new Z-band alternatively spliced PDZ-motif protein. *J. Cell Biol.* 146:465–475.

Flood, G., E. Kanana, A.P. Gilmore, A.J. Rowe, W.B. Graatzer, and D.R. Critchley. 1995. Association of structural repeats in the alpha-actinin rod domain. Alignment of inter-subunit interactions. *J. Mol. Biol.* 252:227–234.

Furst, D.O., and M. Gautel. 1995. The anatomy of a molecular giant: how the sarcomere cytoskeleton is assembled from immunoglobulin superfamily molecules. *J. Mol. Cardiol.* 27:951–959.

Gertler, F.B., K. Niebuhr, M. Reinhard, J. Wehland, and P. Soriano. 1996. Mena, a relative of VASP and *Drosophila enabled*, is implicated in the control of microfilament dynamics. *Cell.* 87:227–239.

Gilmore, A.P., and K. Burridge. 1996. Molecular mechanisms for focal adhesion assembly through regulation of protein–protein interactions. *Structure.* 4:647–651.

Gregorio, C.C., K. Trombitas, T. Centner, B. Kolmerer, G. Stier, K. Kunke, K. Suzuki, F. Obermayr, B. Herrmann, and H. Granzier. 1998. The NH_2 terminus of titin spans the Z-disc: its interaction with a novel 19-kD ligand (T-cap) is required for sarcomeric integrity. *J. Cell Biol.* 143:1013–1027.

Gumbiner, B. 2000. Regulation of cadherin adhesive activity. *J. Cell Biol.* 148: 399–403.

Hance, J.E., S.Y. Fu, S.C. Watkins, A.H. Beggs, and M. Michalak. 1999. Alpha-actinin-2 is a new component of the dystrophin–glycoprotein complex. *Arch. Biochem. Biophys.* 365:216–222.

Hardy, S., M. Kitamura, T. Harris-Stansil, Y. Dai, and M.L. Phipps. 1997. Construction of adenovirus vectors through Cre-lox recombination. *J. Virol.* 71: 1842–1849.

Hungerford, J.E., M.T. Compton, M.L. Matter, B.G. Hoffstrom, and C.A. Otey. 1996. Inhibition of $pp125^{FAK}$ in cultured fibroblasts results in apoptosis. *J. Cell Biol.* 135:1383–1390.

Huttelmaier, S., O. Maybodora, B. Harbeck, T. Jarchau, B.M. Jockusch, and M Rudiger. 1998. The interaction of the cell-contact proteins VASP and vinculin is regulated by phosphatidylinositol-4,5-biphosphate. *Curr. Biol.* 8:479–488.

Kamei, T., G.P. Hamlin, B.M. Chapman, A.L. Burkhardt, J.B. Bolen, and M.J. Soares. 1997. Signaling pathways controlling trophoblast differentiation: src family protein tyrosine kinases in the rat. *Biol. Reprod.* 57:1302–1311.

Kang, F.R., O. Laine, J.R. Rubb, F.S. Southwick, and D.L. Puirch. 1997. Profilin interacts with the gly-pro-pro-pro-pro-pro sequences of vasodilator-stimulated phosphoprotein (VASP): implications for actin-based *Listeria* motility. *Biochem.* 36:8384–8392.

Kocks, C., E. Gouin, M. Tabouret, P. Berche, H. Ohayon, and P. Cossart. 1992. *L. monocytogenes*-induced actin assembly requires *actA* gene product, a surface protein. *Cell.* 68:521–531.

Kozak, M. 1991. An analysis of vertebrate mRNA sequences: intimations of translational control. *J. Cell Biol.* 115:887–903.

Labeit, S., D. Barlow, M. Gautel, T. Gibson, J. Holt, C. Hsieh, U. Francke, K. Leonard, J. Wardale, A. Whiting, and J. Trinick. 1990. A regular pattern of two types of 100-residue motif in the sequence of titin. *Nature.* 345:273–276.

Lazarides, E., and K. Burridge. 1975. α-Actinin: immunofluorescent localization of a muscle structural protein in nonmuscle cells. *Cell.* 6:289–298.

Niebuhr, K., F. Ebel, R. Frank, M. Reinhaard, E. Domann, U.D. Carl, U. Walter, F.B. Gertler, J. Wehland, and T. Chakraborty. 1997. A novel proline-rich motif present in ActA of *Listeria monocytogenes* and cytoskeletal proteins is the ligand for the EVH1 domain, a protein module present in the Ena/VASP family. *EMBO (Eur. Mol. Biol. Organ.) J.* 16:5433–5444.

Noguchi, J., M. Yanagisawa, M. Imamura, Y. Kasuya, T. Sakurai, T. Tanaka, and T. Masaki. 1992. Complete primary structure and tissue expression of chicken pectoralis M-protein. *J. Biol. Chem.* 28:20302–20310.

Ohtsuka, H., H. Yajima, S. Kimura, and K. Maruyama. 1997. Binding of the N terminal fragment of connectin/titin to alpha-actinin as revealed by yeast two-hybrid systems. *FEBS Lett.* 401:65–67.

Okagaki, T., F.E. Weber, D.A. Fischman, K.T. Vaughan, T. Mikawa, and F.C. Reinach. 1993. The major myosin-binding domain of skeletal muscle MyBP-C (C protein) residues in the COOH-terminal, immunoglobulin C2 motif. *J. Cell Biol.* 123:619–626.

Olson, N.J., R.B. Pearson, D.S. Neddleman, M.Y. Hurwitz, B.E. Kemp, and A.R. Means. 1990. Regulatory and structural motifs of chicken gizzard myosin light chain kinase. *Proc. Natl. Acad. Sci. USA.* 7:2284–2288.

Otey, C.A., F.M. Pavalko, and K. Burridge. 1990. An interaction between α-actinin and the β_1 integrin subunit in vitro. *J. Cell Biol.* 111:721–729.

Papa, I., C. Astier, O. Kwiatek, F. Raynaud, C. Bonnal, M.C. Lebart, C. Roustan, and Y. Benyamin. 1999. Alpha actinin-CapZ, an anchoring complex for thin filaments in Z-line. *J. Muscle Res. Cell. Motil.* 20:187–197.

Pavalko, F.M., and S.M. LaRoche. 1993. Activation of human neutrophils induces an interaction between the integrin β2 subunit (CD18) and the actin binding protein α-actinin. *J. Immunol.* 151:3795–3805.

Pavalko, F.M., D.M. Walker, L. Graham, M. Goheen, C.M. Doerschuk, and G.S. Kansas. 1995. The cytoplasmic domain of L-selectin interacts with cytoskeletal proteins via α-actinin: receptor positioning in microvilli does not require interaction with α-actinin. *J. Cell Biol.* 129:1155–1164.

Pomies, P., H.A. Louis, and M.C. Beckerle. 1997. CRP1, a LIM domain protein implicated in muscle differentiation, interacts with α-actinin. *J. Cell Biol.* 139:157–168.

Pomies, P., T. Macalma, and M.C. Beckerle. 1999. Purification and characterization of an alpha-actinin-binding PDZ-LIM protein that is up-regulated during muscle differentiation. *J. Biol. Chem.* 274:29242–29250.

Prehoda, K.E., D.J. Lee, and W.A. Lim. 1999. Structure of the enabled/VASP homology 1 domain–peptide complex: a key component in the spatial control of actin assembly. *Cell.* 97:471–480.

Provost, E., and D.L. Rimm. 1999. Controversies at the cytoplasmic face of the cadherin-based adhesion complex. *Curr. Opin. Cell Biol.* 11:567–572.

Purich, D.L., and F.S. Southwick. 1997. ABM-1 and ABM-2 homology sequences: consensus docking sites for actin-based motility defined by oligoproline regions in *Listeria* ActA surface protein and human VASP. *Biochem. Biophys. Res. Commun.* 231:686–691.

Reinhard, M., M. Halbrugge, U. Scheer, C. Wiegand, B.M. Jockusch, and U. Walter. 1992. The 45/50 kD phosphoprotein VASP purified from human platelets is a novel protein associated with actin filaments and focal contacts. *EMBO (Eur. Mol. Biol. Organ.) J.* 11:2063–2070.

Reinhard, M., C. Giehl, K. Abel, C. Haffner, T. Jarchau, V. Hoppe, B.M. Jockusch, and U. Walter. 1995a. The proline-rich focal adhesion and microfilament protein VASP is a ligand for profilins. *EMBO (Eur. Mol. Biol. Organ.) J.* 14:1583–1589.

Reinhard, M., K. Jouvenal, D. Tripier, and U. Walter. 1995b. Identification, purification and characterization of a zyxin-related protein that binds the focal adhesion and microfilament protein VASP. *Proc. Natl. Acad. Sci. USA.* 92: 7956–7960.

Ridley, A.J., H.F. Paterson, C.L. Johnston, D. Diekmann, and A. Hall. 1992. The small GTP-binding protein rac regulates growth factor-induced membrane ruffling. *Cell.* 70:401–410.

Sadler, I., A.W. Crawford, J.W. Michelsen, and M.C. Beckerle. 1992. Zyxin and cCRP: two interactive LIM domain proteins associated with the cytoskeleton. *J. Cell Biol.* 119:1573–1587.

Salmikangas, P., O-M. Mykkanen, M. Gronholm, L. Heiska, J. Kere, and O. Carpen. 1999. Myotilin, a novel sarcomeric protein with two Ig-like domains, is encoded by a candidate gene for limb-girdle muscular dystrophy. *Hum. Mol. Gen.* 8:1329–1336.

Sampath, R., P.J. Gallagher, and F. Pavalko. 1998. Cytoskeletal interactions with the leukocyte integrin β2 cytoplasmic tail. Activation-dependent regulation of associations with talin and alpha-actinin. *J. Biol. Chem.* 273:33588–33594.

Schultz, J., F. Milpetz, P. Bork, and C.P. Ponting. 1998. SMART, a simple modular architecture research tool: identification of signaling domains. *Proc. Natl. Acad. Sci. USA.* 95:5857–5864.

Smith, G.A., J.A. Theriot, and D.A. Portnoy. 1996. The tandem repeat domain

in the *Listeria monocytogenes* ActA protein controls the rate of actin-based motility, the percentage of moving bacteria, and the localization of vasodilator-stimulated phosphoprotein and profilin. *J. Cell Biol.* 135:647–660.

Sorimachi, H., A. Freiburg, B. Kolmerer, S. Ishiura, G. Stier, C.C. Gregorio, D. Labeit, W.A. Linke, K. Suzuki, and S. Labeit. 1998. Tissue-specific expression and alpha-actinin binding properties of the Z-disc titin: implications for the nature of vertebrate Z-discs. *J. Mol. Biol.* 270:688–695.

Symons, M., J.M. Derry, B. Karlak, S. Jiang, V. Lemahieu, F. McCormick, U. Francke, and A. Abo. 1996. Wiskott-Aldrich syndrome protein, a novel effector for the GFPase CDC42Hs, is implicated in actin polymerization. *Cell.* 84:723–734.

Tollefson, A.E., T.W. Hermiston, and W.S.M. Wold. 1999. Preparation and titration of CsCl-banded adenovirus stock. *In* Methods in Molecular Medicine: Adenovirus Methods and Protocols. W.S.M. Wold, editor. Humana Press, Inc., Totowa, NJ. 1–9.

Vaughan, K.T., F.E. Weber, S. Einheber, and D.A. Fischman. 1993. Molecular cloning of chicken MyBP-H (86kDa protein) reveals conserved immunoglobulin C2 and fibronectin type III motifs. *J. Biol. Chem*. 268:3670–3676.

Williams, A.F., and A.N. Barclay. 1988. A year in the life of the immunoglobulin superfamily: domains for cell surface recognition. *Ann. Rev. Immunol.* 6:381–405.

Wulfkuhle, J.D., I.E. Donina, N.H. Start, R.K. Pope, K.N. Pestonjamasp, M.L. Niswonger, and E.J. Luna. 1999. Domain analysis of supervillin, an F-actin bundling plasma membrane protein with functional nuclear localization signals. *J. Cell Sci.* 112:2125–2136.

Wyszynski, M., J. Lin, A. Rao, E. Nigh, A. Beggs, A.M. Craig, and M. Sheng. 1997. Competitive binding of α-actinin and calmodulin to the NMDA receptor. *Nature.* 385:439–442.

Xia, H., S.T. Winokur, W.-L. Kuo, M.R. Altherr, and D.S. Bredt. 1997. Actinin-associated LIM protein: identification of a domain interaction between PDZ and spectrin-like repeat motifs. *J. Cell Biol.* 139:507–515.

Zeile, W.L., R.C. Condit, J.I. Lewis, D.L. Purich, and F.S. Southwick. 1998. Vaccinia locomotion in host-cells: evidence for the universal involvement of actin-based motility sequences ABM-1 and ABM-2. *Proc. Natl. Acad. Sci. USA*. 95:13917–13922.

Zhou, Q., P. Ruiz-Lozano, M.E. Martone, and J. Chen. 1999. Cypher, a striated muscle-restricted PDZ and LIM domain-containing protein, binds to alpha-actinin-2 and protein kinase C. *J. Biol. Chem*. 274:19807–19813.